J Appl Electrochem (2009) 39:1053–1058
DOI 10.1007/s10800-008-9755-4

ORIGINAL PAPER

Electro-oxidation of methanol on co-deposited Pt-MoO$_x$ prepared by cyclic voltammetry with different scanning potential ranges

Tao Huang · Jihua Zhuang · Aishui Yu

Received: 4 June 2008 / Accepted: 12 December 2008 / Published online: 28 December 2008

Abstract Pt-MoO$_x$ supported on glassy carbon was co-deposited by cyclic voltammetry (CV). The lower limit of potential was fixed at −0.25 V (vs. SCE), whereas the upper limit was adjusted to be 0.0, 0.10, 0.40, 0.60 and 1.0 V. The as-prepared catalysts were characterized by X-ray photoelectron microscopy, scanning electron microscopy and transmission electron microscopy. The results show that Pt-MoO$_x$ particles are uniformly dispersed on the substrate and the agglomerated microparticles are composed of numerous nanoparticles with a size of several nanometers. The catalytic capabilities of Pt-MoO$_x$ for methanol oxidation were examined by CV and chronoamperometry. Electrochemical measurements demonstrate that the catalytic activities and stabilities of Pt-MoO$_x$ prepared in the potential ranges from −0.25 to both 0.60 and 1.0 V were higher than the others, which may due to the higher active surface area, more appropriate Pt/Mo ratio and more preferred Pt crystallographic orientation.

Keywords Pt-MoO$_x$ · Methanol electro-oxidation · Cyclic voltammetry · Chronoamperometry

1 Introduction

In recent years, various electrocatalysts have been investigated in order to enhance methanol oxidation and promote methanol oxidation kinetics [1–4]. Noble metal catalysts intermixed with high surface area inorganic oxides are of considerable interest for methanol electro-oxidation. The oxide is believed to modify the electronic nature of the metal particles, which can affect their chemisorptive and catalytic properties. The enhancement of surface catalytic activity, as well as the large surface area achieved with low loading levels, makes such systems attractive for application in methanol electro-oxidation. Molybdenum oxide (MoO$_x$) has been examined as a potential oxide phase to improve the CO-tolerance. The nonstoichiometric lower valence molybdenum oxide contains five distinct phases, namely the Magneli phases with different compositions between MoO$_3$ and MoO$_2$. These mixed-valence molybdenum oxides have a rutile-type structure with short metal–metal bond distance along the direction of edge sharing, which accounts for their high electronic conductivity. Besides their high electronic conductivities, mixed-valence molybdenum oxides are relatively stable in acid solution and have specific catalytic activity [5, 6].

Pt-MoO$_x$ catalysts have been prepared by chemical routes [7–10] and electrochemical co-deposition methods [11, 12]. With the advantage of high purity of deposits, electrochemical co-deposition could lead to uniform dispersion of Pt microparticles onto molybdenum oxide on a microscopic level. This work aims to investigate the effect of plating potential ranges on the performance of Pt-MoO$_x$ for methanol electro-oxidation. Our approach is to prepare Pt-MoO$_x$ catalysts with different Pt/Mo atomic ratios by the electrochemical co-deposition method with different scanning potential ranges and the catalytic activities of Pt-MoO$_x$ for methanol electro-oxidation in acid media were studied by cyclic voltammetry and chronoamperometry.

T. Huang · J. Zhuang · A. Yu (✉)
Department of Chemistry, Shanghai Key Laboratory of
Molecular Catalysis and Innovative Materials, Fudan University,
200433 Shanghai, China
e-mail: asyu@fudan.edu.cn

2 Experimental

2.1 Pt-MoO$_x$ co-deposition

Electrochemical co-deposition of Pt-MoO$_x$ was carried out on an electrochemical workstation (CHI 660A, CHI company) using a conventional three-electrode electrochemical cell with a platinum foil (12 × 12 mm) as counter electrode and a saturated calomel electrode (SCE, +0.241 V vs. NHE) as reference electrode. A glassy carbon electrode (GC, ϕ 5 mm) sealed by PTFE was used as working electrode for Pt-MoO$_x$ co-deposition; this was polished with 0.05 μm alumina powder until a shiny, mirror-like surface was obtained and then ultrasonicated for several minutes in deionized water. The GC electrode was further cleaned in 0.5 M H_2SO_4 solution by electrochemical cyclic voltammetry with the potential range from −0.25 to 1.20 V at a scan rate of 0.05 V s^{-1}. Pt-MoO$_x$ catalysts supported on GC electrodes were prepared by cyclic voltammetry in a solution of 2 mM potassium hexachloroplatinate (IV), 10 mM sodium molybdate and 0.5 M sulfuric acid with scanning potential ranges −0.25 to 0.0, −0.25 to 0.10, −0.25 to 0.40, −0.25 to 0.60, and −0.25 to 1.0 V, at a scan rate of 0.05 V s^{-1} for 20 cycles, and the as-deposited catalysts were sequentially labelled as catalyst ①, ②, ③, ④ and ⑤, respectively.

2.2 Characterization

The as-prepared Pt-MoO$_x$ catalysts were characterized by scanning electron microscopy (SEM), transmission electron microscopy (TEM) and X-ray photoelectron spectroscopy (XPS). SEM images were obtained on a Philips XL 30 with an operating voltage of 20 kV and TEM was performed on a JOEL JEM-2010 electron microscope with an accelerating voltage of 200 kV. XPS experiments were carried out on a RBD upgraded PHI-5000 C ESCA system (Perkin Elmer) with Mg Kα radiation ($h\nu = 1253.6$ eV) or Al Kα radiation ($h\nu = 1486.6$ eV).

2.3 Electrochemical measurements

The as-prepared Pt-MoO$_x$ catalysts were firstly characterized in 0.5 M H_2SO_4 solution at a scan rate of 0.05 V s^{-1} by cyclic voltammetry and their electrochemical performance for methanol oxidation was studied by the means of cyclic voltammetry and chronoamperometry. The cyclic voltammetry measurements were carried out in 0.5 M H_2SO_4 and 0.5 M CH_3OH at a scan rate of 0.05 V s^{-1}, and for chronoamperometry tests, the working electrodes were polarized at 0.60 V in the same solution for 600 s. The electrochemical test results were normalized with per unit active surface area of catalyst. Before each test the solution was purged with N_2 for 15 min and all the electrochemical experiments were performed at room temperature.

3 Results and discussion

3.1 Electrochemical co-deposition of Pt-MoO$_x$ and electrochemical characterization

Figure 1 presents the cyclic voltammograms (CVs) of a GC electrode in a solution of 2 mM K_2PtCl_6, 10 mM Na_2MoO_4 and 0.5 M H_2SO_4 with different scanning potential ranges at a scan rate of 0.05 V s^{-1} for 20 cycles. The reduction peak at −0.18 V in the negative-going potential scan is attributed to the reduction of Pt (IV) to Pt and the redox peaks at 0.02 and 0.18 V can be assigned to oxidation/reduction of MoO_2/MoO_3 [11, 13]. The peak current densities (except the one at −0.18 V) increase with increasing cycle number, which implies growth of Pt-MoO$_x$ catalysts on the GC surface. After 20 cycles, the Pt-MoO$_x$/GC electrodes were removed from the solution and washed with deionized water.

The as-prepared Pt-MoO$_x$ catalysts were characterized in 0.5 M H_2SO_4 solution at a scan rate of 0.05 V s^{-1}. Figure 2 shows the comparison of CV curves of catalyst ①, ②, ③, ④ and ⑤. In the potential range from −0.25 to 0.10 V, there are two pairs of redox peaks around −0.15 and 0.0 V. The redox current peaks at −0.15 V are related to hydrogen adsorption/desorption on the crystal surface (110) sites of Pt and the pair of current peaks around 0.0 V are attributable to hydrogen adsorption/desorption on (100) sites. It is well known that the number of adsorption sites on faces (100), (111) and (110) of Pt are 4, 3 and 5, respectively [14, 15], which means that face (110) is the most favorable orientation. The results showed that the current density of methanol oxidation at −0.15 V is in order of catalyst ⑤ ≈ ④ > ③ > ② > ①, which indicates that both catalyst ⑤ and ④ have much more crystal face (110) sites of Pt than the other three. The redox peaks at 0.0 V give the same order as of −0.15 V, which means that numbers of Pt(100) sites for catalyst ④ and ⑤ are also more than the others. This difference may be one of the elements for different catalytic activities for methanol oxidation. The larger amount of adsorption sites could lead to better catalytic behavior for methanol electro-oxidation.

The electrochemical active surface area (S) of Pt-MoO$_x$ catalysts can be calculated from the electrical charge of hydrogen adsorption/desorption integrated from the CV curves.

$$S = \frac{Q}{Q_{\mathrm{H}}^{0}} \qquad (1)$$

where Q is the total electrical charge of the hydrogen adsorption, and Q_{H}^{0} is the charge for monolayer hydrogen

Fig. 1 Cyclic voltammograms for GC electrodes in 2 mM K_2PtCl_6, 10 mM Na_2MoO_4, and 0.5 M H_2SO_4 with different scanning potential ranges, scan rate: 0.05 V s^{-1}, cycling number is 20 cycles

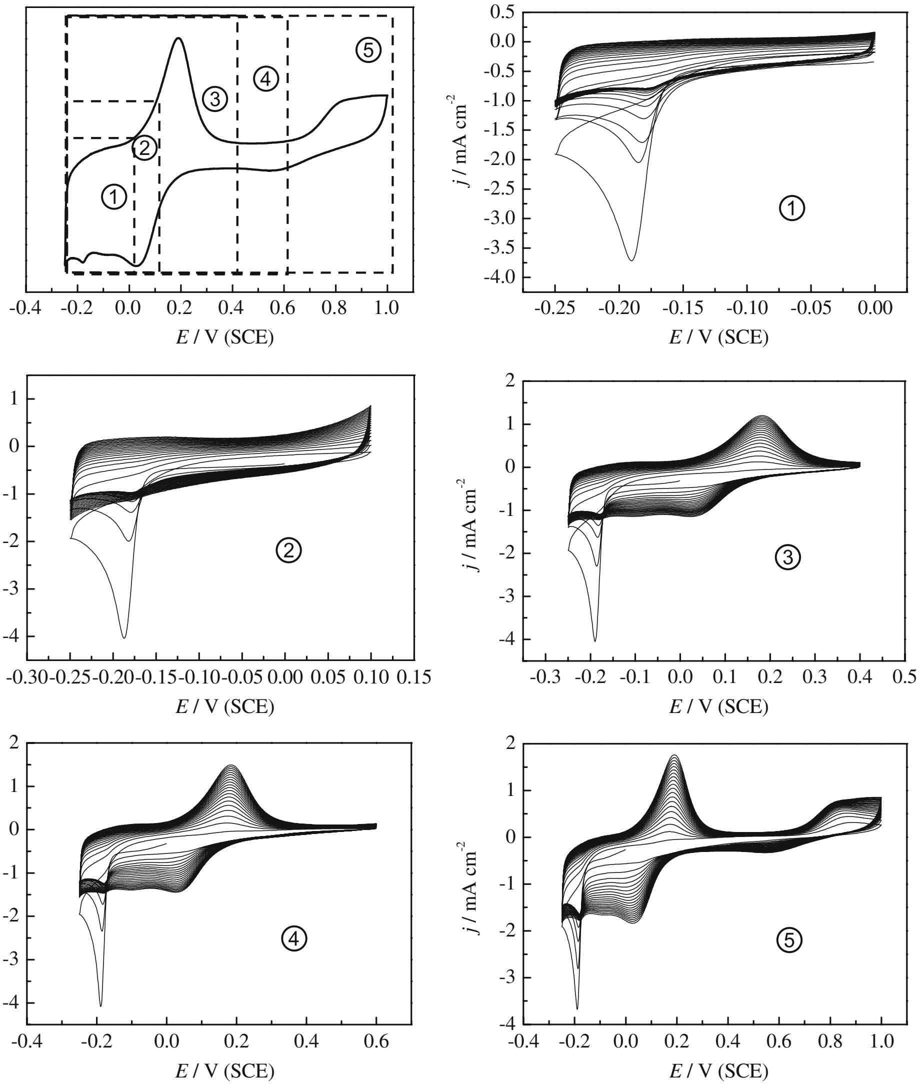

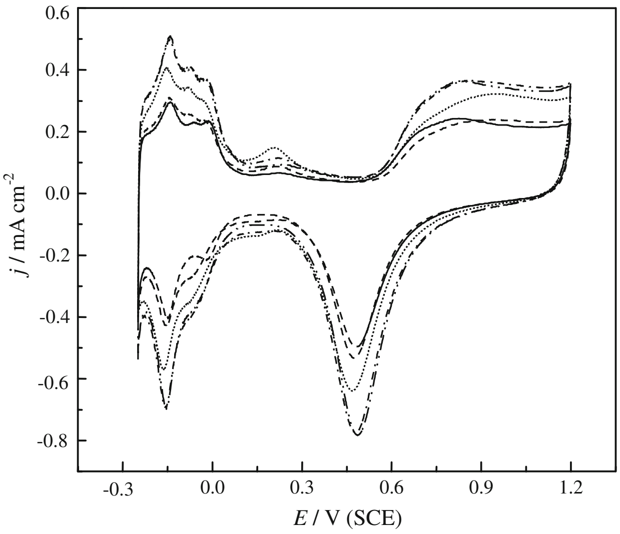

Fig. 2 Cyclic voltammograms of different Pt-MoO_x/GC electrodes in 0.5 M H_2SO_4 solution. ———— Catalyst ①, - - - - Catalyst ②, ····· Catalyst ③, - · - · - Catalyst ④ and – ·· – Catalyst ⑤

adsorption on Pt (i.e. 210 μC cm^{-2}) [10, 16]. From CV curves, the integrated electrical charges of the hydrogen adsorption are 94.0, 96.2, 127.0, 157.6 and 164.4 μC for catalysts ①, ②, ③, ④ and ⑤ and the calculated electrochemical active surface areas are 0.448, 0.458, 0.605, 0.750 and 0.782 cm^2, respectively. Catalysts ④ and ⑤ have similar active surface areas which are higher than the others. Clearly, the upper limit of scanning potential has a significant effect on the active surface area of Pt-MoO_x. With increase of the upper limit of scanning potential, the active surface area of Pt-MoO_x increases.

3.2 Surface characterization

SEM images of the as-prepared Pt-MoO_x/GC electrodes are presented in Fig. 3. Pt-MoO_x microparticles are uniformly dispersed on GC substrate with agglomeration of microparticles. From the TEM image (Fig. 4), it can be clearly seen that the agglomerated microparticles are composed of

Fig. 3 SEM images of different Pt-MoO$_x$/GC electrodes with a magnification of 20,000. **a** Catalyst ①, **b** Catalyst ②, **c** Catalyst ③, **d** Catalyst ④, **e** Catalyst ⑤

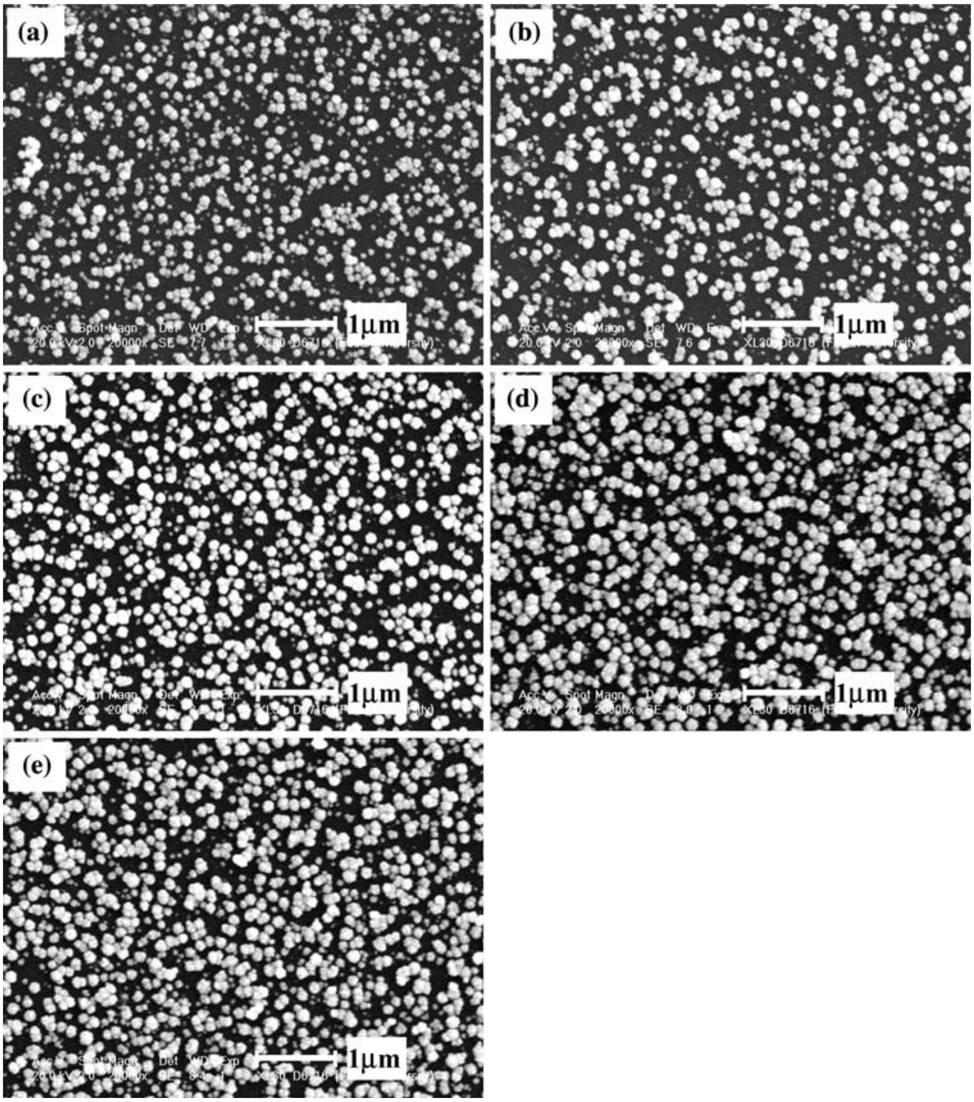

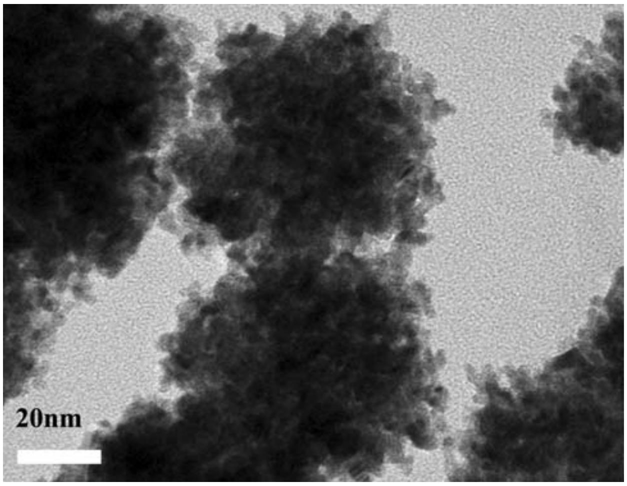

Fig. 4 TEM image of agglomerated particles of Pt-MoO$_x$

Table 1 Pt/Mo atomic ratio on the surface of Pt-MoO$_x$ catalyst calculated from XPS measurements

	Plating potential range (V)	Atomic ratio of Pt to Mo
Catalyst ①	−0.25 to 0.0	0.58:1
Catalyst ②	−0.25 to 0.1	0.67:1
Catalyst ③	−0.25 to 0.4	1.12:1
Catalyst ④	−0.25 to 0.6	7.90:1
Catalyst ⑤	−0.25 to 1.0	8.31:1

numerous nanoparticles with a size of several nanometers. The agglomeration increases slightly with the upper limit of scanning potential during electrochemical co-deposition. The Pt/Mo atomic ratios of the as-prepared Pt-MoO$_x$ catalysts determined by XPS are listed in Table 1. The atomic ratios of Pt to Mo increase with the upper limit of scanning potential, which, for catalyst ① is 0.58, whereas it is 8.31 for catalyst ⑤. The higher Pt content on the electrode surface may be the reason for the relatively higher surface area, as discussed in Sect. 3.1. Although the upper limit of scanning potential has little effect on the morphology of Pt-MoO_x, it greatly affects the Pt/Mo atomic ratio of the catalyst.

3.3 Electrochemical oxidation of methanol

Figure 5 presents cyclic voltammograms of methanol electro-oxidation on different Pt-MoO_x catalysts in a solution of 0.5 M CH_3OH and 0.5 M H_2SO_4 expressed by current (Fig. 5a) and current density (current/active surface area, Fig. 5b). The onset potentials for methanol electro-oxidation are all around 0.18 V. In the forward scan, methanol oxidation produced a symmetrical anodic peak at 0.62 V and an anodic peak at 0.42 V in the reverse scan, which is attributable to the reduction of the oxidized Pt oxide and the removal of the incompletely oxidized carbonaceous species formed in the forward scan [17–19]. The ratio of the forward anodic peak current density (j_f) to the reverse anodic peak current density (j_b), j_f/j_b, can be used to describe the catalyst tolerance to carbonaceous species accumulation [20]. A low j_f/j_b ratio indicates poor oxidation of methanol to carbon dioxide during the anodic scan and excessive accumulation of carbonaceous residues on the electrode surface. The ratios of j_f/j_b are 1.12, 1.16, 1.18, 1.14 and 1.10 for catalyst ①, ②, ③, ④ and ⑤, respectively. These five catalysts have a close ratio of j_f/j_b, which means they have similar tolerance to carbonaceous species, however the ranks of current (in Fig. 5a) and current density (Fig. 5b) are both in the order ⑤ ≈ ④ > ③ > ② > ①. The plots of current density versus time for methanol electrochemical oxidation at 0.60 V on different Pt-MoO_x/GC catalysts with the method of chronoamperometry are compared in Fig. 6. These curves reflect the activities and stabilities of different catalysts for methanol electro-oxidation. Obviously, catalyst ⑤ has the highest initial current and limiting current density, which indicates its best catalytic activity and stability for methanol oxidation. The limiting current density is in order ⑤ ≈ ④ > ③ > ② > ①, which is consistent with the CV results presented in Fig. 5. The catalytic activity of Pt-MoO_x catalyst for methanol electro-oxidation is dependent on its active surface area and Pt/Mo atomic ratio (Fig. 6).

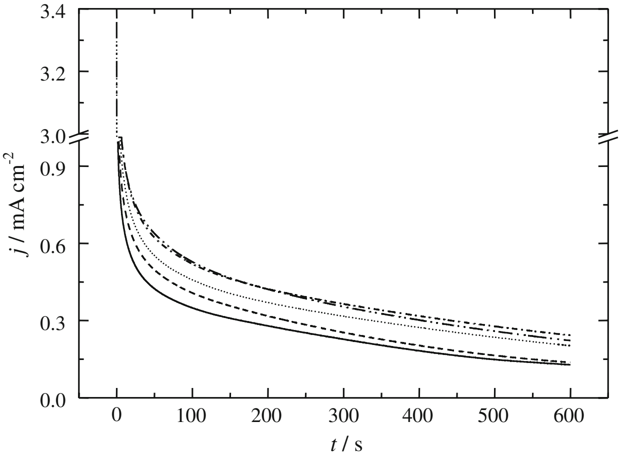

Fig. 6 Chronoamperometry measurements of methanol oxidation in a solution of 0.5 M CH_3OH and 0.5 M H_2SO_4 on Pt-MoO_x/GC electrodes at 0.60 V. ———— Catalyst ①, - - - - Catalyst ②, ····· Catalyst ③, - · - · - Catalyst ④ and – ·· – Catalyst ⑤

4 Conclusions

The plating potential ranges in cyclic voltammetric co-deposition of Pt-MoO_x catalysts have important effects on the catalytic activities for methanol oxidation. The composition and active surface area of Pt-MoO_x catalysts can be modified by adjusting the scanning potential ranges. With increasing of the upper limit of scanning potential, the prepared catalyst gave more preferred Pt crystallographic orientation, higher active surface area and higher Pt/Mo atomic ratio; therefore better electrochemical performance for methanol electro-oxidation.

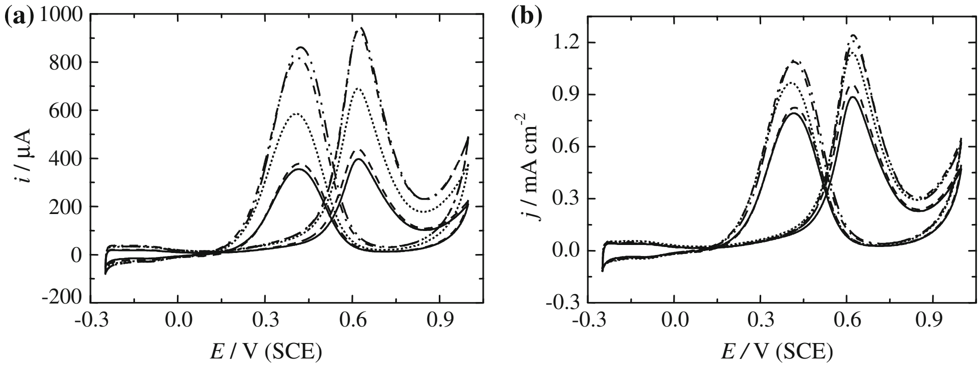

Fig. 5 Cyclic voltammograms of Pt-MoO_x/GCs in 0.5 M CH_3OH and 0.5 M H_2SO_4. ———— Catalyst ①, - - - - Catalyst ②, ····· Catalyst ③, - · - · - Catalyst ④ and – ·· – Catalyst ⑤

References

1. Dyer CK (2002) J Power Sources 106:31
2. Dillon R, Srinivasan S, Aricò AS et al (2004) J Power Sources 127:112
3. Gebel G, Diat O (2005) Fuel Cells 5:261
4. Winter M, Brodd RJ (2004) Chem Rev 104:4245
5. Zhang H, Wang Y, Fachini ER et al (1999) Electrochem Solid State Lett 2:437
6. Chen G, Wang ZY, Xia DG (2004) Electrochem Commun 6:268
7. Ioroi T, Fujiwara N, Siroma Z et al (2002) Electrochem Commun 4:442
8. Ioroi T, Yasuda K, Siroma Z et al (2003) J Electrochem Soc 150:A1225
9. Miyazaki K, Matsuoka K, Iriyama Y et al (2005) J Electrochem Soc 152:A1870
10. Ioroi T, Akita T, Yamazaki S et al (2006) Electrochim Acta 52:491
11. Wang Y, Fachini ER, Cruz G et al (2001) J Electrochem Soc 148:C222
12. Gan YP, Huang H, Zhang WK (2007) Trans Nonferrous Met Soc China 17:214
13. Machida K, Enyo M (1990) J Electrochem Soc 137:1169
14. Kinoshita K (1990) J Electrochem Soc 137:845
15. Stoyanova A, Naidenov V, Petrov K et al (1999) J Appl Electrochem 29:1197
16. Tran TD, Langer SH (1993) Anal Chem 65:1805
17. Xu WL, Lu TH, Liu CP et al (2005) J Phys Chem B 109:14325
18. Zhu J, Su Y, Cheng FJ et al (2007) J Power Sources 166:331
19. Manoharan R, Goodenough JB (1992) J Mater Chem 2:875
20. Zhao GY, Xu CL, Guo DJ et al (2006) J Power Sources 162:492